

Rapidity distribution of photons from an anisotropic *Quark-Gluon-Plasma*

Lusaka Bhattacharya^a and Pradip Roy^b

Saha Institute of Nuclear Physics

1/AF Bidhannagar, Kolkata - 700064, INDIA

ABSTRACT

We calculate rapidity distribution of photons due to Compton and annihilation processes from *Quark Gluon Plasma* (QGP) with pre-equilibrium momentum-space anisotropy. We also include contributions from hadronic matter with late stage transverse expansion. A phenomenological model has been used for the time evolution of hard momentum scale $p_{\text{hard}}(\tau)$ and anisotropy parameter $\xi(\tau)$. As a result of pre-equilibrium momentum-space anisotropy, we find significant modification of photons rapidity distribution. For example, with *fixed initial condition* (FIC) *free-streaming* ($\delta = 2$) interpolating model we observe significant enhancement of photon rapidity distribution at fixed p_T , where as for FIC *collisionally-broadened* ($\delta = 2/3$) interpolating model the yield increases till $y \sim 1$. Beyond that suppression is observed. With *fixed final multiplicity* (FFM) *free-streaming* interpolating model we predict enhancement of photon yield which is less than the case of FIC. Suppression is always observed for FFM *collisionally-broadened* interpolating model.

1 Introduction

Relativistic heavy ion colliders (RHIC), at Brookhaven National Laboratory and upcoming Large Hadron Collider (LHC) at CERN, are designed to produce and study strongly interacting matter at high temperature and/or density. Experiments at the RHIC have already demonstrated that high p_T hadrons in central $A + A$ collisions are significantly suppressed in comparison with that in binary scaled $p + p$ collisions [1]. This observation has been referred to as *jet-quenching* which clearly indicates towards the formation of *Quark Gluon Plasma* (QGP)³ at the RHIC experiments. Another most important task is to characterize different properties of this new state of matter, such as isotropization/thermalization.

The most difficult problem lies in the determination of isotropization and thermalization time scales (τ_{iso} and τ_{therm})⁴. Studies on elliptic flow (upto about $p_T \sim 1.5 - 2$ GeV) using

^aE-mail address: lusaka.bhattacharya@saha.ac.in

^bE-mail address: pradipk.roy@saha.ac.in

³Theoretically QGP is expected to be formed when the temperature of nuclear matter is raised above its critical value, $T_c \sim 170$ MeV, or equivalently the energy density of nuclear matter is raised above $1 \text{ GeV}/\text{fm}^3$

⁴From now on we will concentrate on the most simplest possibility that is both the time-scale are the same, $\tau_{\text{therm}} = \tau_{\text{iso}}$.

ideal hydrodynamics indicate that the matter produced in such collisions becomes isotropic with $\tau_{\text{iso}} \sim 0.6 \text{ fm/c}$ [2, 3, 4]. On the contrary, perturbative estimates yield much slower thermalization of QGP [5]. However, recent hydrodynamical studies [6] have shown that due to the poor knowledge of the initial conditions, there is a sizable amount of uncertainty in the estimation of thermalization or isotropization time. The other uncertain parameters are the transition temperature T_c , the spatial profile, and the effects of flow. Thus it is necessary to find suitable probes which are sensitive to these parameters. Electromagnetic probes have long been considered to be one of the most promising tools to characterize the initial state of the collisions [7, 8]. Because of the very nature of their interactions with the constituents of the system they tend to leave the system without much change of their energy and momentum. Photons (dilepton as well) can be one of such observables.

But, photons can carry information about the plasma initial conditions [9, 10, 11] only if the observed flow effects from the late stages of the collisions can be understood and modeled properly. The observation of pronounced transverse flow in the photon transverse momentum distribution has been taken into account in model calculations of photon p_T distribution at various beam energies [9, 10, 12, 13, 14]. It is found that because of the transverse kick the low energy photons populate the intermediate regime and consequently, the contribution from hadronic matter becomes comparable with that from the hadronic matter destroying the window where the contribution from QGP was supposed to dominate [14]. Apart from transverse flow effects, the investigation of longitudinal evolution using HBT correlation measurements has been done in Ref. [15]. It is shown that the decrease of R_{side} with p_T ($> 2.5 \text{ GeV}$) provides a good indication whether transverse flow is significant or not. But, so far as the pre-equilibrium emission is concerned this effect is not important. However, in the late stage, transverse expansion becomes important and we include this while estimating the photon yield from the hadronic matter.

Photon (dilepton) production from relativistic heavy-ion collisions has been extensively studied in Ref. [16, 17, 18, 19]. All these works are based on the assumption of rapid thermalization of plasma with $\tau_{\text{therm}} = \tau_i$, where τ_i is the time scale of plasma formation. However, due to rapid longitudinal expansion of the plasma at early time this assumption seems to be very drastic because it ignores the momentum space anisotropy developed along the beam axis.

The phenomenological consequences of early stage pre-equilibrium momentum space anisotropy of QGP have been studied in Ref. [20, 21] in the context of dileptons and in Ref. [22, 23] in the context of photons. In Ref. [22] the effects of time-dependent momentum-space anisotropy of QGP on the medium photon production are discussed. It is shown that the introduction of early time momentum-space anisotropy can enhance the photon production yield significantly. Also the present authors calculate transverse momentum distribution of direct photons from various sources by taking into account the initial state momentum anisotropy of QGP and the late stage transverse flow effects [23]. The total photon yield is compared with the recent measurement of photon transverse momentum distribution by the PHENIX Collaboration to extract the isotropization time [23]. It is found that the data can be reproduced with τ_{iso} in the range $0.5 - 1.5 \text{ fm/c}$. All these works show that the introduction of pre-equilibrium momentum space anisotropy has significant effect on the medium dilepton as well as photon productions. In the present work, we will be investigating the rapidity dependence of thermal photon in the presence of pre-equilibrium momentum space

anisotropy. The importance of rapidity distributions of photons and dileptons produced in relativistic heavy ion collisions has been previously realized in Ref. [24, 25, 26]. As for example, fluctuations in the rapidity distributions can signal a phase transition, a supercooling of the fluid, or the presence of quark-matter bubbles, etc. Moreover, it was shown in Ref. [15] that photon rapidity density can be a good probe to distinguish between Landau-like [27] and Bjorken-like [28] dynamics. Therefore, photon rapidity density should carry the signatures of pre-equilibrium momentum space anisotropy. The rapidity distribution of thermal photons produced in $Pb + Pb$ collisions at CERN SPS is also demonstrated in Ref. [29] using a three-fluid hydrodynamical model. It is argued that rapidity dependence of photon spectra can provide cleaner insight about the rapidity dependence of the initial conditions, e. g. the temperature/time.

In absence of any precise knowledge about the dynamics at early time of the collision, one can introduce phenomenological models to describe the evolution of the pre-equilibrium phase. In this work, we will use one such model, proposed in Ref. [20], for the time dependence of the anisotropy parameter, $\xi(\tau)$, and hard momentum scale, $p_{\text{hard}}(\tau)$. This model introduces four parameter to parameterize the ignorance of pre-equilibrium dynamics: the parton formation time (τ_i), the isotropization time (τ_{iso}), which is the time when the system starts to undergo ideal hydrodynamical expansion and γ sets the sharpness of the transition to hydrodynamical behavior. The fourth parameter δ is introduced to characterize the nature of pre-equilibrium anisotropy i.e whether the pre-equilibrium phase is non-interacting or collisionally broadened. The phenomenological model in Ref. [20] assumes Bjorken's boost invariant expansion of the plasma. Therefore, this leads to a rapidity independent production of thermal photons. One can easily see that this can not be true for collisions involving nuclei having a finite energy. The experimental data are expected to be better described by rapidity dependent parton distribution functions. Therefore, in this work, we have used rapidity dependent quark and anti-quark distribution functions. The rapidity dependence of the distribution functions arises from the rapidity dependence of the initial temperature, $T_i(\eta)$.

The organization of the paper is as follows. In the next section (section 2) we shall discuss the mechanisms of photon production rate using an anisotropic phase space distribution along with the space-time evolution of the matter. Results are presented in section 3 and finally we conclude in section 4.

2 Formalism

2.1 Photon rate : Anisotropic QGP

The lowest order mechanisms for photon emission from QGP are the Compton ($q(\bar{q})g \rightarrow q(\bar{q})\gamma$) and the annihilation ($q\bar{q} \rightarrow g\gamma$) processes. The rate of photon production from anisotropic plasma due to Compton and annihilation processes has been calculated in Ref. [30]. The soft contribution is calculated by evaluating the photon polarization tensor for an oblate momentum-space anisotropy of the system where the cut-off scale is fixed at $k_c \sim \sqrt{g}p_{\text{hard}}$. Here p_{hard} is a hard-momentum scale that appears in the distribution functions.

The differential photon production rate for $1 + 2 \rightarrow 3 + \gamma$ in an anisotropic medium is

given by [30]:

$$E \frac{dR}{d^3p} = \frac{\mathcal{N}}{2(2\pi)^3} \int \frac{d^3p_1}{2E_1(2\pi)^3} \frac{d^3p_2}{2E_2(2\pi)^3} \frac{d^3p_3}{2E_3(2\pi)^3} f_1(\mathbf{p}_1, p_{\text{hard}}(\tau, \eta), \xi) f_2(\mathbf{p}_2, p_{\text{hard}}(\tau, \eta), \xi) \\ \times (2\pi)^4 \delta(p_1 + p_2 - p_3 - p) |\mathcal{M}|^2 [1 \pm f_3(\mathbf{p}_3, p_{\text{hard}}(\tau, \eta), \xi)] \quad (1)$$

where, $|\mathcal{M}|^2$ represents the spin averaged matrix element squared for one of those processes which contributes in the photon rate and \mathcal{N} is the degeneracy factor of the corresponding process. ξ is a parameter controlling the strength of the anisotropy with $\xi > -1$. f_1 , f_2 and f_3 are the anisotropic distribution functions of the medium partons and will be discussed in the following. Here it is assumed that the infrared singularities can be shielded by the thermal masses for the participating partons. This is a good approximation at times short compared to the time scale when plasma instabilities start to play an important role.

The anisotropic distribution function can be obtained [31] by squeezing or stretching an arbitrary isotropic distribution function along the preferred direction in the momentum space,

$$f_i(\mathbf{p}, \xi, p_{\text{hard}}) = f_i^{\text{iso}}(\sqrt{\mathbf{p}^2 + \xi(\mathbf{p} \cdot \mathbf{n})^2}, p_{\text{hard}}(\tau, \eta)) \quad (2)$$

where \mathbf{n} is the direction of anisotropy. It is important to notice that $\xi > 0$ corresponds to a contraction of the distribution function in the direction of anisotropy and $-1 < \xi < 0$ corresponds to a stretching in the direction of anisotropy. In the context of relativistic heavy ion collisions, one can identify the direction of anisotropy with the beam axis along which the system expands initially. The hard momentum scale p_{hard} is directly related to the average momentum of the partons. In the case of an isotropic QGP, p_{hard} can be identified with the plasma temperature (T).

2.2 Photon rate: Hadronic matter

Photons are also produced from different hadronic reactions from hadronic matter either formed initially (no QGP scenario) or realized as a result of a phase transition (assumed to be first order in the present work) from QGP. Photons from hadronic reactions and decays cannot be calculated in a model-independent way. The hadronic matter produced in heavy ion collisions is usually considered to be a gas of the low lying mesons π , ρ , ω , η and nucleons. Reactions between these as well as the decays of the ρ and ω were considered to be the sources of thermal photons from hadronic matter [7, 18, 32].

We follow the calculations done in Ref. [33] where convenient parameterizations have been given for the reactions considered. These parameterizations will be used while doing the space-time evolution to calculate the photon yield from meson-meson reactions.

2.3 Space time evolution

The rate given in Eq. (1) is the static rate which has to be convoluted with the space-time history of the plasma to obtain phenomenologically predictable quantities, for example, $dN/d^2p_T dy$ for a given p_T or $dN/d^2p_T dy$ for a given y . In our calculation, we assume an

isotropic plasma is formed at initial temperature T_i and initial time (proper) τ_i . Subsequent rapid expansion of the matter along the longitudinal direction causes faster cooling in the beam direction than in the transverse direction. As a result the system becomes anisotropic and remains so till $\tau = \tau_{\text{iso}}$.

The exact dynamics at the early-stage of the heavy ion collision is almost unknown. Thus, a precise theoretical picture of the evolutions of p_{hard} and ξ is not possible. However, we can always introduce phenomenological models to parameterize the ignorance. In this work, we shall closely follow the work of Ref. [21] to evaluate the rapidity distribution of photons from the first few Fermi of the plasma evolution. Three scenarios of the space-time evolution (as described in Ref. [21]) are the following: (i) $\tau_{\text{iso}} = \tau_i$, the system evolves hydrodynamically so that $\xi = 0$ and p_{hard} can be identified with the temperature (T) of the system (till date all the calculations have been performed in this scenario), (ii) $\tau_{\text{iso}} \rightarrow \infty$, the system never comes to equilibrium, (iii) $\tau_{\text{iso}} > \tau_i$ and τ_{iso} is finite, one should devise a time evolution model for ξ and p_{hard} which smoothly interpolates between pre-equilibrium anisotropy and hydrodynamics. We shall follow scenario (iii) (see Ref. [21] for details) in which case the time dependence of the anisotropy parameter ξ is given by

$$\xi(\tau, \delta) = \left(\frac{\tau}{\tau_i}\right)^\delta - 1 \quad (3)$$

where the exponent $\delta = 2$ ($2/3$) corresponds to *free-streaming* (*collisionally-broadened*) pre-equilibrium momentum space anisotropy and $\delta = 0$ corresponds to complete isotropization. As in Ref. [21], a transition width γ^{-1} is introduced to take into account the smooth transition from non-zero value of δ to $\delta = 0$ at $\tau = \tau_{\text{iso}}$. The time dependence of various quantities are, therefore, obtained in terms of a smeared step function [20]:

$$\lambda(\tau) = \frac{1}{2}(\tanh[\gamma(\tau - \tau_{\text{iso}})/\tau_i] + 1). \quad (4)$$

For $\tau \ll \tau_{\text{iso}}$ ($\gg \tau_{\text{iso}}$) we have $\lambda = 0(1)$ which corresponds to *free-streaming* (hydrodynamics). With this, the time dependence of relevant quantities are as follows [21, 26]:

$$\begin{aligned} \xi(\tau, \delta) &= \left(\frac{\tau}{\tau_i}\right)^{\delta(1-\lambda(\tau))} - 1, \\ p_{\text{hard}}(\tau, \eta) &= T_i(\eta) \bar{\mathcal{U}}^{1/3}(\tau), \end{aligned} \quad (5)$$

where,

$$\begin{aligned} \mathcal{U}(\tau) &\equiv \left[\mathcal{R} \left(\left(\frac{\tau_{\text{iso}}}{\tau} \right)^\delta - 1 \right) \right]^{3\lambda(\tau)/4} \left(\frac{\tau_{\text{iso}}}{\tau} \right)^{1-\delta(1-\lambda(\tau))/2}, \\ \bar{\mathcal{U}} &\equiv \frac{\mathcal{U}(\tau)}{\mathcal{U}(\tau_i)}, \\ \mathcal{R}(x) &= \frac{1}{2} [1/(x+1) + \tan^{-1} \sqrt{x}/\sqrt{x}] \end{aligned} \quad (6)$$

and T_i is the initial temperature of the plasma.

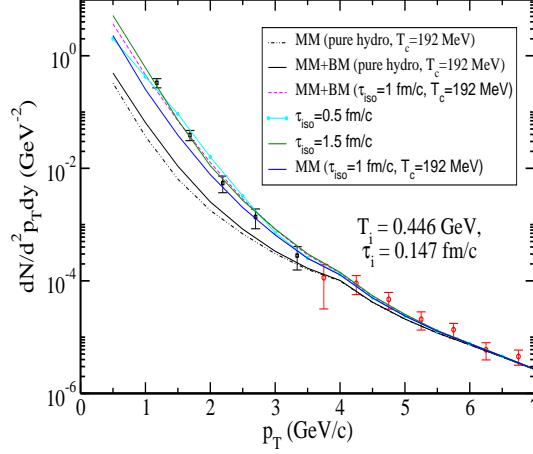


Figure 1: (Color online) Photon transverse momentum (p_T) distributions at RHIC energy with initial condition $T_i = 0.446$ GeV and $\tau_i = 0.147$ fm/c. MM (BM) represents the contribution from meson-meson (baryon-meson) interactions (see [23] for details).

To estimate the initial conditions we assume that i.e the longitudinal expansion approximately follows the scaling law, $v_z = z/t$, we can relate the initial density to the final multiplicity distribution by

$$n_i \tau_i = \frac{1}{\pi R_\perp^2} \frac{dN}{d\eta} \quad (7)$$

and the initial temperature (T_i) is related with the initial density by the following relation.

$$n_i = \frac{\zeta(3)g_Q}{\pi^2} T_i^3 \quad (8)$$

where g_Q is degeneracy factor. The multiplicity distribution can be parameterized as

$$\frac{dN}{d\eta} = \left(\frac{dN}{d\eta} \right)_0 \exp \left(-\frac{\eta^2}{2\sigma^2} \right) \quad (9)$$

where $(dN/d\eta)_0$ is the total multiplicity at $\eta = 0$ and $\sigma = 3(5)$ for RHIC (LHC) energies. The initial temperature is therefore a function of η , i. e $T_i = T_i(\eta)$.

So far, we have discussed the evolution during early stage only. For ($\tau > \tau_{\text{iso}}$) we propose that τ_{iso} onward the system is described by $(1+2)d$ ideal hydrodynamics. As the system becomes isotropic at $\tau = \tau_{\text{iso}}$, $p_{\text{hard}}(\tau_{\text{iso}})$ and τ_{iso} can be identified as the initial conditions, i. e., initial temperature and initial time for the hydrodynamic evolution. The initial conditions for ideal hydrodynamics is given by,

$$\begin{aligned} T_i^{\text{hydro}} &= p_{\text{hard}}(\tau_{\text{iso}}) \\ \tau_i^{\text{hydro}} &= \tau_{\text{iso}} \end{aligned} \quad (10)$$

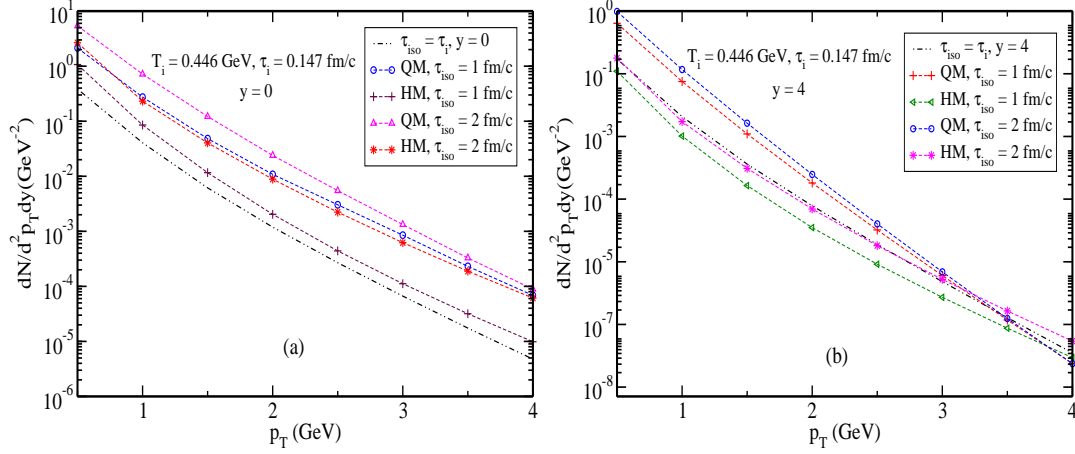


Figure 2: (Color online) The p_T distribution of photons for FIC *free-streaming* ($\delta = 2$) interpolating model at RHIC energy at (a) $y = 0$ and (b) $y = 4$.

Eventually the system undergoes a phase transition (assumed to be first order in the present work) at $\tau = \tau_f$, where τ_f is determined by the condition $p_{\text{hard}}(\tau = \tau_f) = T_c$, where $T_c \sim 170$ MeV. The phase transition ends at $\tau_H = r_d \tau_f$, where $r_d = g_Q/g_H$ is the ratio of the degrees of freedom in the two (QGP phase and hadronic phase) phases. Therefore, the total photon yield, arising from present scenario is given by the following equation,

$$\frac{dN}{d^2p_T dy} = \left[\int d^4x E \frac{dR}{d^3p} \right]_{\text{aniso}} + \left[\int d^4x E \frac{dR}{d^3p} \right]_{\text{hydro}}, \quad (11)$$

where the first term denotes the contribution from the anisotropic QGP phase and the second term represents the contributions evaluated in ideal hydrodynamics scenario. The rapidity density is defined as,

$$\frac{dN}{dy} = \int d^2p_T \frac{dN}{dy d^2p_T} \quad (12)$$

In order to numerically compute the integrals in Eqs. (11) and (12), one needs to know the time dependence of p_{hard} and ξ which has been discussed earlier.

After introducing the space-time evolution of relevant quantities, we are now completely equipped for the integration of Eqs. (11) and (12). However, before going into the details of rapidity distributions of photons at the heavy ion collider experiments like RHIC and LHC, let us concentrate on few interesting features of the phenomenological model introduced for the evolution of $p_{\text{hard}}(\tau, \eta)$ and $\xi(\tau)$.

The simple model, introduced in section 2.3, which smoothly interpolates between an initially non-equilibrium plasma to an isotropic plasma, is based on the assumption that the initial conditions are held fixed. The smooth interpolation (keeping the initial condition fixed) between anisotropic and isotropic phases (described in section 2) results into a hard momentum scale (for $\tau \gg \tau_{\text{iso}}$) which is by a factor $[\mathcal{R}((\tau_{\text{iso}}/\tau_i)^\delta - 1)]^{0.25}$ larger compared to

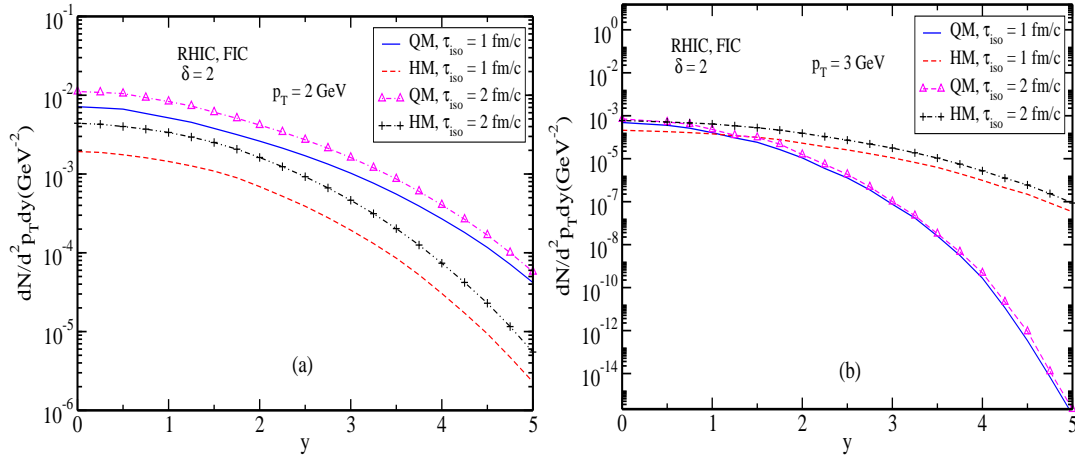


Figure 3: (Color online) Rapidity distribution (y) of photon at RHIC energy from quark matter (QM) and hadronic matter (HM) for (a) $p_T = 2$ GeV and (b) $p_T = 3$ GeV.

the momentum scale results from the hydrodynamic expansion of a system (with the same initial condition) from the beginning (see Eqs. (5) and (6)). As a consequence of this enhancement of $p_{\text{hard}}(\tau, \eta)$, the *fixed initial condition* interpolating models (both *free-streaming* and *collisionally-broadened*) will result in generation of particle number during the transition from non-equilibrium to equilibrium phase. Moreover, the entropy generation increases with the increasing value of τ_{iso} . Thus, the requirement of bounded entropy generation can be used to put some upper bound on the value of τ_{iso} for *fixed initial condition* interpolating models. As for example, if we allow maximum 20% entropy generation at RHIC, the maximum possible value of τ_{iso} will be 1.2 (18) fm/c for *fixed initial condition collisionally-broadened* (*free-streaming*) interpolating model.

Due to the phenomenological constraints on the entropy generation, one might not allow any entropy generation at all. In that case, one can redefine $\bar{\mathcal{U}}(\tau)$ in Eq. (5) to ensure *fixed final multiplicity* in this model. Since we know the amount of enhancement (which is responsible for this entropy generation) of p_{hard} , the redefinition of $\bar{\mathcal{U}}(\tau)$ will be straight forward [21]:

$$\bar{\mathcal{U}}(\tau) = \mathcal{U}(\tau) \left[\mathcal{R}((\tau_{\text{iso}}/\tau_i)^\delta - 1) \right]^{-3/4} (\tau_i/\tau_{\text{iso}}) \quad (13)$$

It is important to mention that this redefinition corresponds to a lower initial temperature ($p_{\text{hard}}(\tau_i, \eta) < T_i$) for $\tau_{\text{iso}} > \tau_i$. Larger value of isotropization time corresponds to lower initial temperature.

2.4 Photon rapidity distribution for fixed p_T

The rapidity distribution of photons at fixed p_T from a QGP or hadronic matter can be obtained by integrating Eq. (11). We use a Monte-Carlo computer code to numerically evaluate Eq. (11). For RHIC energies the formation time is taken as $\tau_i = 0.147$ fm/c.

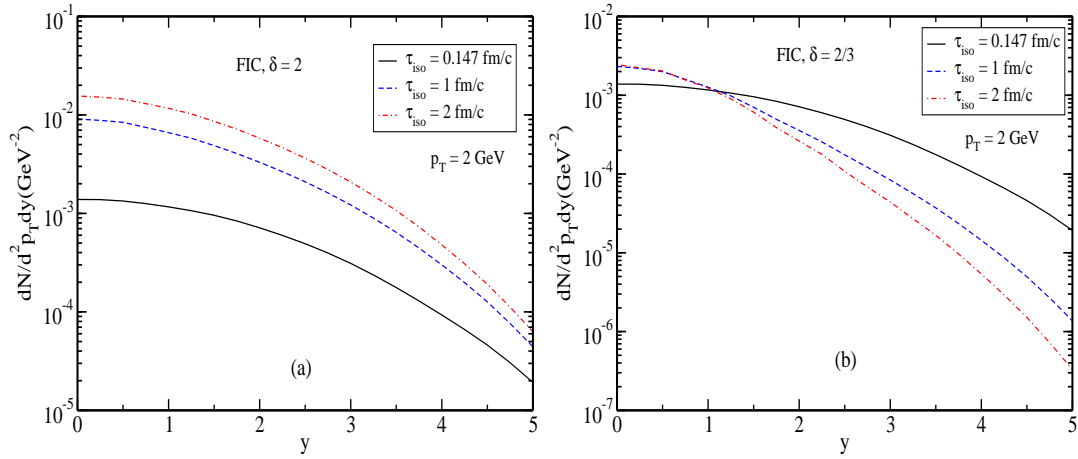


Figure 4: (Color online) Photon rapidity distribution at RHIC energy for FIC interpolating model, at $p_T = 2$ GeV for (a) $\delta = 2$ and (b) $\delta = 2/3$.

This corresponds to an initial temperature of $T_i = 446$ MeV at $\eta = 0$ [19]. For the LHC energies, we assume the formation time to be $\tau_i = 0.073$ fm/c and the initial temperature to be $T_i = 897$ MeV at $\eta = 0$.

As a consequence of pre-equilibrium momentum-space anisotropy, significant modification of the thermal photon rapidity distribution is expected. To quantify the effect of isotropization time on the rapidity distribution of the thermal photons, we define *photon modification* factor $\Phi(y, \tau_{\text{iso}})|_{p_T}$ for fixed p_T as the ratio of photon yields with and without pre-equilibrium momentum-space anisotropy,

$$\Phi(y, \tau_{\text{iso}})|_{p_T} = \left(\frac{dN(y, \tau_{\text{iso}})}{dy d^2 p_T} \right)_{p_T} / \left(\frac{dN(y, \tau_{\text{iso}} = \tau_i)}{dy d^2 p_T} \right)_{p_T} \quad (14)$$

The modification factor Φ is not measurable quantity. If there is an anisotropy in nature, the numerator can be measured (see Eq. 14). If there is no anisotropy in nature the denominator can be measured. But it is impossible to measure both simultaneously. However, Φ is a useful quantity only for demonstrative purpose.

3 Results

Before going to the description of photon rapidity distribution, we validate the present model in the context of PHENIX photon data [35]. It has already been demonstrated in Ref. [23]. We shall repeat here for completeness.

To show the presence of initial state momentum anisotropy, we plot the total photon yield assuming hydrodynamic evolution from the very beginning as well as with finite τ_{iso} in Fig. 1. It is clearly seen that some amount of anisotropy is needed to reproduce the data. We note that the value of τ_{iso} needed to describe the data lies in the range $0.5 \text{ fm/c} \leq \tau_{\text{iso}} \leq 1.5 \text{ fm/c}$, independent of values of the transition temperatures [23]. It is to be noted that observables

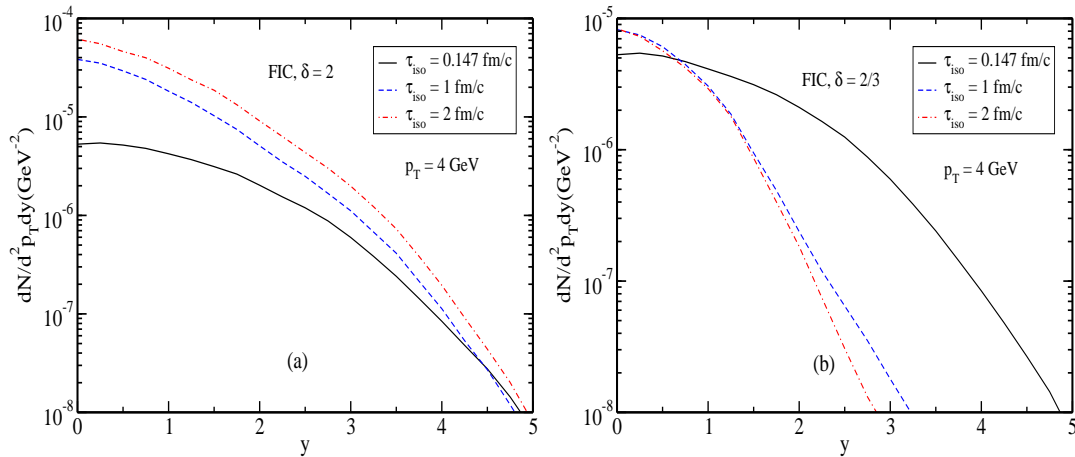


Figure 5: (Color online) Photon rapidity distribution at RHIC energy for FIC interpolating model, at $p_T = 4$ GeV for (a) $\delta = 2$ and (b) $\delta = 2/3$.

like photon p_T distribution along with the ratio of photon to pion rapidity density will further strengthen the validity of the present model.

3.1 Fixed initial condition (FIC) interpolating model

Fixed initial condition (FIC) interpolating models always result into an enhanced value of hard momentum scale as a consequence of pre-equilibrium anisotropy. This feature of this model has already been discussed briefly before (see Ref. [21] for details). As a consequence of this enhancement of p_{hard} , pre-equilibrium anisotropy increases the density of plasma partons with small rapidities. However, for higher rapidities, this enhancement is complemented by the suppression arising from the non-zero value of anisotropy parameter ξ . The anisotropic parton distribution function in Eq. (2) clearly suggests that for the positive values of ξ , parton density decreases if we decrease the angle between the momentum of partons and the direction of anisotropy. From the very beginning, we have assumed that pre-equilibrium momentum-space anisotropy (in the heavy ion collisions) results from the rapid longitudinal expansion of the system immediately after the collision. Thus, in the context of relativistic heavy ion collision, one can identify the direction of anisotropy as the beam axis. Moreover, due to the rapid longitudinal cooling (as a consequence of rapid longitudinal expansion), one always finds oblate anisotropic distributions i.e positive value of ξ . Therefore, introduction of pre-equilibrium anisotropy with fixed initial condition increases the density of plasma partons moving in the transverse direction [22] and at the same time decreases the density of plasma partons moving in the forward direction. This feature of fixed initial condition pre-equilibrium momentum-space anisotropy should be reflected in the photon rapidity distribution which we will discuss in the following.

As a consequence of this enhancement of partons moving in the transverse direction and suppression of partons moving in forward direction, we expect an enhancement of the yield

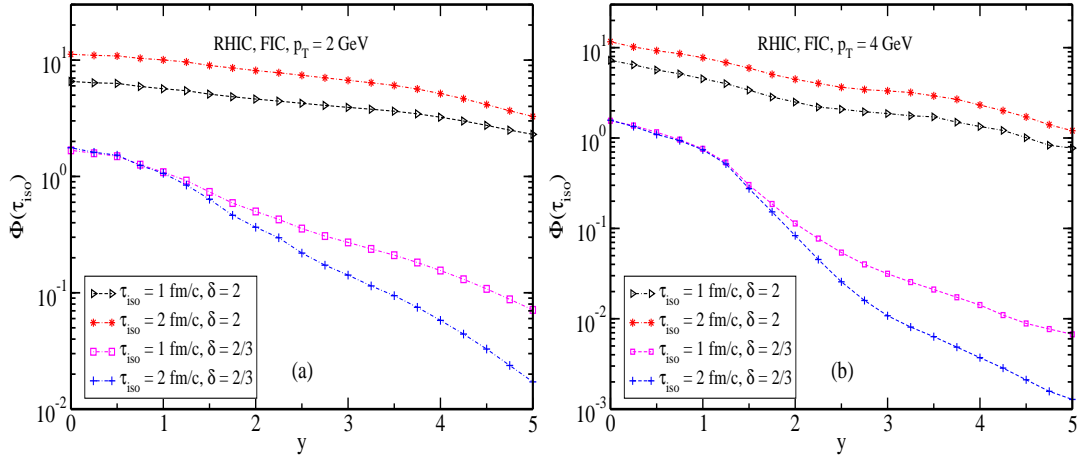


Figure 6: (Color online) Modification factor for FIC interpolating model at RHIC energy, (a) $p_T = 2$ GeV and (b) $p_T = 4$ GeV.

in the transverse direction ($y = 0$)⁵ and suppression in the longitudinal direction ($y \neq 0$).

To see the relative importance of the contributions from quark matter (QM) and hadronic matter (HM) we evaluate the p_T distribution of photons for fixed rapidity from the evolving fireball. Because the effect of transverse flow is pronounced in the late stages of the collisions we neglect this effect in the early stage and include it during the late stage. For $\tau \geq \tau_{\text{iso}}$, the system is described by ideal relativistic hydrodynamics in $(1+2)d$ [36] with longitudinal boost invariance [28] and cylindrical symmetry. Therefore, the total thermal photon yield for fixed y , arising from the present scenario (FIC interpolating model) is given by Eq. (11).

To elucidate the effect of transverse expansion, we first show results in the frame work of FIC *free-streaming* ($\delta = 2$) interpolating model. In Fig. 2 we have plotted the p_T distribution of photons for two different isotropization time ($\tau_{\text{iso}} = 1$ and 2 fm/c) at (a) $y = 0$ and (b) $y = 4$. Both Figs. 2a and 2b clearly suggest that for $1 \leq p_T \leq 4$ GeV, the photons from the quark matter (QM) dominates over the hadronic matter (HM). As we increase the isotropization time (τ_{iso}) from 1 to 2 fm/c (see Fig. 2), both the contributions from quark matter and hadronic matter increases. However, quark matter contributions still dominate over hadronic matter contributions. Therefore, for the above mentioned p_T range, the effects of pre-equilibrium momentum space anisotropy will be much more prominent irrespective of isotropization time (τ_{iso}). In support of this argument, we have plotted $dN/d^2p_T dy$ as a function of rapidity (y) for fixed p_T ($p_T = 2$ GeV) in Fig. 3a for two different values of isotropization time ($\tau_{\text{iso}} = 1$ and 2 fm/c respectively). Fig. 3a shows that the contributions from hadronic matter are always smaller than the contributions from the quark matter. However, for $p_T = 3$ GeV, QM and HM contributions are of similar magnitude for $y \leq 1$ (see Fig. 3b). Beyond that the HM contributions dominates.

The feature described above is better understood by looking at Figs. 4 and 5 where the total contributions have been plotted. In Fig. 4, we have presented the rapidity distribution

⁵This feature was already established in our previous work [22].

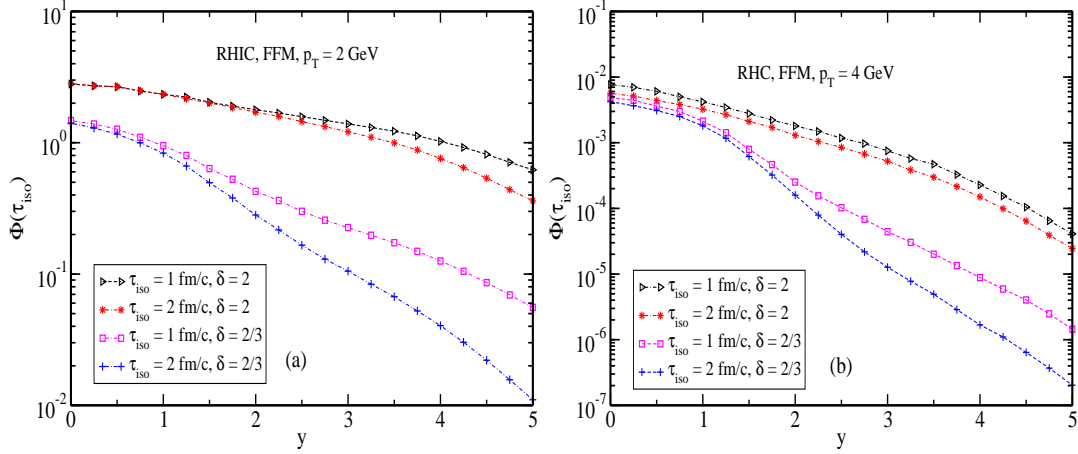


Figure 7: (Color online) Modification factor for FFM interpolating model at RHIC energy, (a) $p_T = 2$ GeV, (b) $p_T = 4$ GeV.

of photons ($dN/d^2p_T dy$) as a function of rapidity (y) with fixed transverse momentum $p_T = 2$ GeV (for three different values of isotropization time, $\tau_{\text{iso}} = \tau_i$, 1 and 2 fm/c) in the framework of *fixed initial condition* for (a) *free-streaming* ($\delta = 2$) and (b) *collisionally-broadened* ($\delta = 2/3$) interpolating models. The rapidity distribution of photons with $p_T = 4$ GeV are presented in Fig. 5 for (a) *free-streaming* ($\delta = 2$) and (b) *collisionally-broadened* ($\delta = 2/3$) interpolating model. Figs. 4a and 5a show enhancements of photon yields (for the FIC *free-streaming* ($\delta = 2$)) interpolating model) in the low rapidity region ($0 \leq y \leq 5$). Marginal suppressions in the higher rapidity region ($y \geq 5$) are observed. The situation is different for the FIC *collisionally broadened* ($\delta = 2/3$) interpolating model (see Figs. 4b and 5b) which shows slight enhancements of photon yields in the low rapidity region ($0 \leq y \leq 1.5$) and suppressions for the rest of the rapidity region ($y \geq 1.5$). This can be attributed to the fact that in the case of *collisionally-broadened interpolating* model we have included the possibility of momentum space broadening of the plasma partons due to interactions. As a consequence the hard momentum scale p_{hard} (which is related to the average momentum in the partonic distribution functions) decreases with time, whereas for *free-streaming* model, the hard momentum scale remains unchanged ($p_{\text{hard}}(\tau) = p_{\text{hard}}(\tau_i) = T_i$, for $\tau < \tau_{\text{iso}}$) upto $\tau = \tau_{\text{iso}}$.

These enhancement and suppression are more clearly revealed from Fig. 6 which shows the *modification factors* for (a) $p_T = 2$ GeV and (b) $p_T = 4$ GeV. For a better comparison of *free-streaming* and *collisionally-broadened* pre-equilibrium phases, we have plotted the *modification factors* for $\delta = 2$ and $2/3$ in the same graph.

We always find enhancement (one order of magnitude) for $\delta = 2$. The trend of the graph shows that at larger rapidities ($y > 5$) the yield will be suppressed for the FIC *free-streaming* ($\delta = 2$) interpolating model. However, we observe suppression for FIC *collisionally-broadened* interpolating model at rapidities $y \geq 1.5$. These findings are similar to that in Ref. [22] where for $\delta = 2$ with FIC considerable enhancement is observed at $y = 0$. But for $\delta = 2/3$, it is found that the enhancement is small.

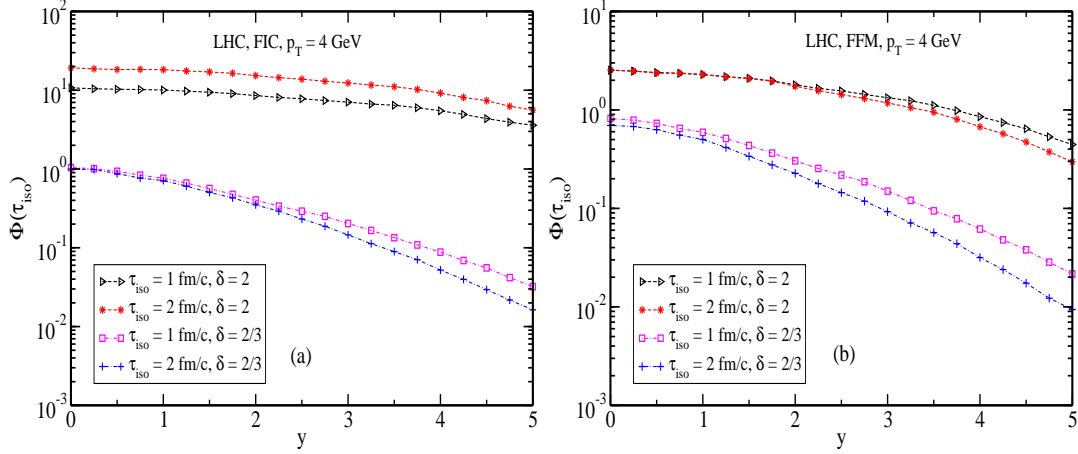


Figure 8: (Color online) Modification factors, (a) FIC and (b) FFM interpolating models at LHC energy at $p_T = 4$ GeV.

3.2 Fixed final multiplicity (FFM) interpolating model

The problems, regarding the entropy generation (appears in *fixed initial condition* model), could be eliminated by enforcing *fixed final multiplicity*. However, enforcing *fixed final multiplicity* corresponds to a lower value of initial hard momentum scale ($p_{\text{hard}}(\eta) < T_i(\eta)$). Moreover, in this case, the initial hard momentum scale will be isotropization time dependent i.e larger the value of τ_{iso} lower will be the initial hard momentum scale. The suppression of hard momentum scale corresponds to a suppression in the plasma parton density compared to the *fixed initial condition* interpolating model. Therefore, for *fixed final multiplicity* interpolating model, we predict more suppression in the photon yield compared to the FIC interpolating model. As a consequence of non-zero positive anisotropy parameter ξ , photons with higher rapidities will be more suppressed.

These features (compared to *fixed initial condition* interpolating model) can be better understood by looking at the *modification factors* for *fixed final multiplicity* interpolating model displayed in Fig. 7 for (a) $p_T = 2$ GeV and (b) $p_T = 4$ GeV at RHIC energy. For $\delta = 2$ (see Fig. 7a) enhancement is observed for the rapidity range upto $y \leq 4$ GeV. After that ($y \geq 4$), we observe the suppression of the photon yield. But for $\delta = 2/3$ (see the same Fig), we observe slight enhancement of the photon yield upto $y \leq 1.5$ and suppression for the rest of the rapidity region. For $\delta = 2/3$ at lower rapidities the rate is close to unity and as we go to higher rapidities the rate is reduced. It is to noted that although, in the case of FFM interpolating model, we have started with a lower value of initial hard momentum scale ($p_{\text{hard}}(\tau_i) \leq T_i(\tau_i)$), we obtain an enhancement in the low rapidity region (Fig. 7a) at $p_T = 2$ GeV for both $\delta = 2$ and $2/3$ respectively. For higher p_T (4 GeV) the yield is suppressed at all rapidities irrespective of the values of δ (Fig. 7b). However, the amount of suppression, for $\delta = 2/3$ at rapidities $y \geq 2$, is large compared to the *free-streaming* pre-equilibrium phase ($\delta = 2$). For a more realistic case ($\delta = 2/3$) the suppression is by a factor of 0.85 which is in accordance with Ref. [26] for the case of dilepton.

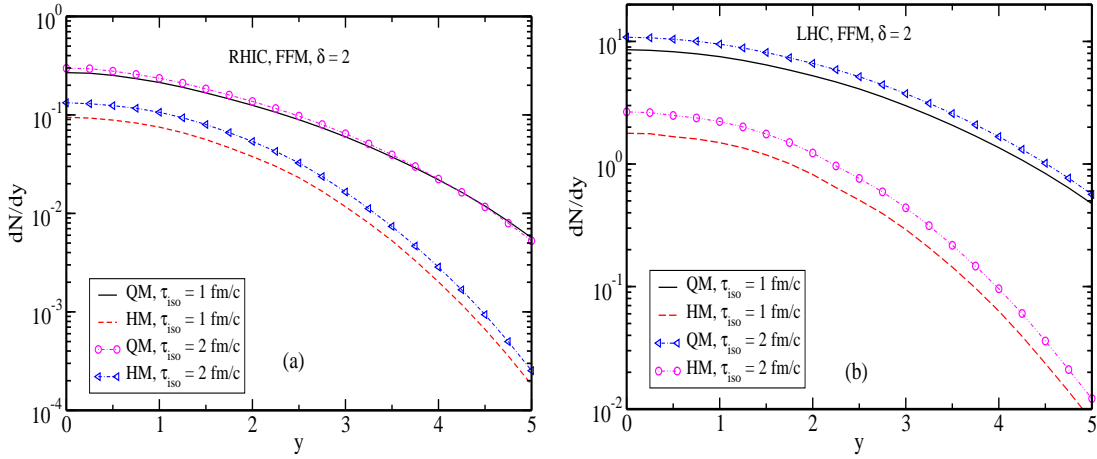


Figure 9: (Color online) Photon rapidity density at (a) RHIC and (b) LHC energies for FFM *free-streaming* ($\delta = 2$) interpolating models.

In Fig. 8, we have presented the *photon modification* factor for $p_T = 4$ GeV as a function of photon rapidity for $\sqrt{s_{NN}} = 5.5$ TeV. Fig. 8a shows enhancement (suppression) for *free-streaming* (*collisionally-broadened*) pre-equilibrium phase for FIC. On the other hand, for FFM model (see Fig. 8b), we obtain suppression for *collisionally-broadened* pre-equilibrium phase. For *free-streaming* pre-equilibrium phase, we find small enhancement in the lower rapidity region and suppression for higher rapidities.

3.3 Photon rapidity density

There is one more phenomenologically interesting observable namely the photon rapidity density, dN/dy , which is defined in Eq. (12). Its shape at least is not expected to be affected by the transverse expansion of the system. Therefore, this quantity is phenomenologically very relevant. We have assumed two different values of isotropization time ($\tau_{\text{iso}} = 1, 2$ fm/c) to compute the rapidity density of photons from an anisotropic QGP. Since the detection of very soft photons is experimentally challenging, photons having their transverse momentum greater than 1 GeV is considered.

The consequences of pre-equilibrium momentum-space anisotropy (with *fixed initial condition* and *fixed final multiplicity*) on the photon production have already been discussed in section 3.1 and 3.2 in details.

We show the effects of transverse expansion to the rapidity density in Fig. 9, where we have plotted the individual contributions of photon rapidity density from the quark matter (QM) and the hadronic matter (HM) in the frame work of *free-streaming* ($\delta = 2$) FFM interpolating model at (a) RHIC and (b) LHC energies. As we vary τ_{iso} from 1 to 2 fm/c (in both the Figs. 9a and 9b), the individual contributions from the quark matter and the hadronic matter increase. At the same time rapidity density of photons from the quark matter is higher than the contributions from the hadronic matter. This is true for the RHIC as well as LHC energies (see Fig. 9). This result is consistent with Fig. 3.

Let us now mention the main features of our observations. With FIC for both values of δ we see moderate enhancement at not too large rapidities. Similar feature has been noted earlier [22]. This can be attributed to the fact that momentum anisotropy enhances the density of plasma partons in the transverse direction. However, it is also to be noted that for larger rapidities the rate is suppressed for both the values of δ . This is due to the fact that the density of partons with higher longitudinal momentum (larger y) decreases. It is worthwhile to mention that the effects of pre-equilibrium momentum space anisotropy for $\delta = 2$ is more compared to that for $\delta = 2/3$. This is because $\delta = 2/3$ corresponds to close to isotropization. With FFM we observe marginal enhancement at low rapidities but considerable suppression at higher rapidities for both *free-streaming* and *collisionally-broadened* interpolating models. This suppression can be described in two ways. Due to rapid longitudinal expansion the distribution function becomes anisotropic. Photons with the larger values of longitudinal momentum are reduced compared with the photons with isotropic distribution function. Maximum amount of momentum-space anisotropy achieved in the early times will be the important cause of the suppression. The suppression will also depend on the time dependence of the anisotropy parameter ξ . Another source of rapidity dependence is given by hard momentum scale (p_{hard}) which depends on the initial temperature (T_i) and hence on rapidity. So we see that the hard momentum scale is directly related with the η even in the case of instantaneous thermalization and satisfies the relation in Eq. (5).

It is important to mention that photon rapidity density significantly depends on the expansion dynamics of the system. In absence of any theoretical knowledge, one can introduce different models for the expansion dynamics of the system like, Bjorken and Landau dynamics etc. In Ref. [15], it is shown that different expansion scenarios predicts different shape for photon rapidity density and thus, the shape of photon rapidity density can be used to distinguish different expansion scenarios. It is argued that the actual expansion scenario lies between Bjorken and Landau hydrodynamics by using various photonic observables [15].

In this article, we have only concentrated on the thermal photon rapidity (from both the quark matter and the hadronic matter) density as a probe of pre-equilibrium anisotropy. However, there are other non-thermal sources of photon like, hard photons, fragmentation photons, decay photons etc. Hard photons are produced in the initial hard scattering of colliding nuclei and are insensitive to the later stage evolution of the QGP. Therefore, they do not carry any information about the pre-equilibrium anisotropy. Similarly, fragmentation and decay photons are also not sensitive to the pre-equilibrium phase. It is to be mentioned that apart from thermal photons from quark matter, thermal photons are also produced from hot hadronic matter where the late stage transverse expansion plays important role. In this work we include this effects of late stage transverse expansion. There is another important source of photons namely, the photons from jet-plasma interaction. The importance of jet-plasma interaction in the context of PHENIX [35] photon data was shown in Ref. [19]. For jet-plasma interaction, the jet-parton distribution functions do not depend on the pre-equilibrium phase. However, the plasma parton densities depend on the pre-equilibrium anisotropy. Therefore, the jet-plasma interaction is sensitive to the pre-equilibrium anisotropy. However, the sensitivity is smaller compared to the thermal photons. Because, for thermal photons, both the initial state partons are sensitive to the anisotropy. Moreover, the jet-photon contribution dominates over the thermal photon contribution only in the high p_T region. Therefore, pho-

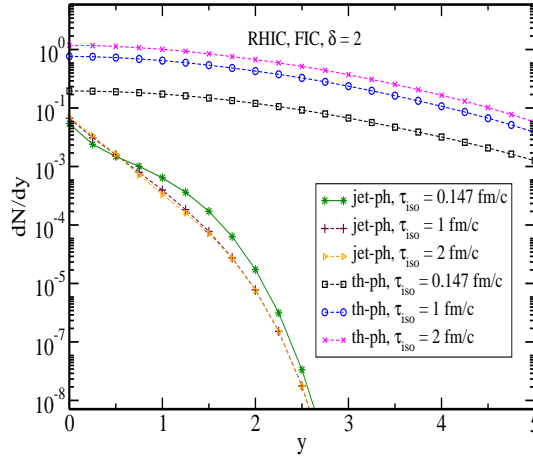


Figure 10: (Color online) thermal photon and jet-photon rapidity density at RHIC energy for FIC *free-streaming* ($\delta = 2$) interpolating model.

tons from jet-plasma interaction insignificantly contributes to the photon rapidity density in the p_T range considered here.

In Fig. 10, we have plotted the contribution from jet plasma interaction along with the anisotropic contributions for two values of isotropization times in the frame work of FIC *free-streaming* interpolating model. We have also presented the contribution from isotropic QGP (i.e. corresponding thermal photon rapidity density) in the same figure for comparison. It is seen that the contribution from jet-plasma interaction is well below the anisotropic contribution, leaving behind a window - where the effects of anisotropy could be seen. Fig. 10 clearly shows that jet-photon contribution is not very significant in the context of thermal photon rapidity density.

4 Conclusion

To summarize, we have investigated the effects of the pre-equilibrium momentum space anisotropy of the QGP along with the effects of late stage transverse expansion on the $p_T(y)$ distribution at fixed $y(p_T)$ and rapidity density (dN/dy) of photons. To describe space-time evolution of hard momentum scale, $p_{\text{hard}}(\tau)$ and anisotropy parameter, $\xi(\tau)$, phenomenological models have been used [21]. These phenomenological models assume the existence of an intermediate time scale called the isotropization time (τ_{iso}). The first model is based on the assumption of fixed initial condition. However, enforcing fixed initial condition causes entropy generation. Therefore, we have also considered another model, which assumes the fixed final multiplicity. Both the possibilities of *free-streaming* and *collisionally-broadened* pre-equilibrium phase of the QGP are considered. The rapidity distribution of photons for different isotropization times in the frame work of these phenomenological models have been estimated. We observed that, for fixed initial condition, a *free streaming* interpolating model can enhance the photon yield significantly for rapidities upto $y \sim 4.5$. However,

for *collisionally-broadened* pre-equilibrium phase with fixed initial condition, the enhancement of photon yield is upto $y \sim 1.5$. After that we observe the suppression of the photon yield for the entire rapidity region ($y \geq 1.5$). Since fixing the final multiplicity reduces the initial hard momentum scale or equivalently the initial energy density, we observe slight enhancement in the low rapidity region and significant suppression (both for the *free-streaming* and *collisionally-broadened* interpolating models) for the rest of the rapidity region. This suppression can be explained as a consequence of the combined effect of the anisotropy in momentum-space achieved at early times due to expansion and the rapidity dependence of the hard momentum scale. For RHIC energies at $p_T = 2$ GeV, QM contribution dominates over the HM contribution. However, for $p_T = 3$ GeV, the later dominates over QM for $y \leq 1$. But as far as the total contribution is concerned, we always find significant modification (enhancement or suppression depending upon the initial conditions used) of the yield in presence of pre-equilibrium momentum space anisotropy.

The other observables like heavy-quark transport [37], jet-medium-induced electromagnetic and gluonic radiation could be phenomenologically very useful in order to detect the consequences of pre-equilibrium momentum-space anisotropy.

Acknowledgments: We would like to thank D. K. Srivastava and S. Sarkar for their useful suggestions.

References

- [1] K. Adcox et al. (PHENIX Collaboration), Phys. Rev. Lett. **88**, 022301 (2001); C. Adler et al. (STAR Collaboration), Phys. Rev. Lett. **89**, 202301 (2002); M. Gyulassy and X. Wang, Nucl. Phys. B **420**, 583 (1994).
- [2] P. Huovinen, P. Kolb, U. Heinz, and P. V. Ruuskanen, Phys. Lett. B **503**, 58 (2001).
- [3] T. Hirano and K. Tsuda, Phys. Rev C **66** 054905 (2002).
- [4] M. J. Tannenbaum, Rept. Prog. Phys. **69** 2005 (2006).
- [5] R. Baier, A. H. Muller, D. Schiff and D. T. Son, Phys. Lett. B **502**, 51 (2001).
- [6] M. Luzum and P. Romatschke, arXiv:0804.4015 [nucl-th].
- [7] J. Alam, S. Sarkar, P. Roy, T. Hatsuda, and B. Sinha, Ann. Phys. **286** 159 (2001).
- [8] J. Alam, S. Raha and B. Sinha, Phys. Rep. **273** 243 (1996).
- [9] J. Alam, J. K. Nayak, P. Roy, A. K. Dutt-Mazumder, and B. Sinha, J. Phys. G **34**, 871 (2007).
- [10] D. K. Srivastava, Eur. Phys. J. C **10**, 487 (1999).
- [11] P. Houvinen, P. V. Ruuskanen, and S. S. Rasanen, Phys. Lett. B **535**, 109 (2002).

- [12] J. Cleymens, K. Redlic, and D. K. Srivastava, Phys. Rev. C **55**, 1431 (1997).
- [13] J. Alam, S. Sarkar, T. Hatsuda, T. K. Nayak, and B. Sinha, Phys. Rev. C **63**, 021901(R) (2001).
- [14] T. Renk, hep-ph/0408218.
- [15] T. Renk, Phys. Rev. C **71**, 064905 (2005).
- [16] S. Sarkar, J. Alam, P. Roy, A. K. Dutt-Mazumder, B. Dutta-Roy, and B. Sinha, Nucl. Phys. A **634** 206 (1998).
- [17] P. Roy, S. Sarkar, J. Alam, and B. Sinha, Nucl. Phys. A **653** 277 (1999).
- [18] J. Kapusta, P. Lichard, and D. Seibert, Phys. Rev. D **44** 2774 (1999).
- [19] S. Turbide, C. Gale, S. Jeon and G. D. Moore, Phys. Rev. C **72**, 014906 (2005).
- [20] M. Martinez and M. Strickland, Phys. Rev. Lett **100**, 102301 (2008).
- [21] M. Martinez and M. Strickland, Phys. Rev C **78**, 034917 (2008).
- [22] L. Bhattacharya and P. Roy, Phys. Rev. C **78**, 064904 (2008).
- [23] L. Bhattacharya and P. Roy, Phys. Rev. C **79**, 054910 (2009).
- [24] S. Sarkar, D. K. Srivastava and B. Sinha, Phys. Rev. C **51**, 318 (1995).
- [25] R. Vogt, B. V. Jacak, P. L. McGaughey and P. V. Ruuskanen, Phys. Rev. D **49**, 3345 (1994).
- [26] M. Martinez and M. Strickland, Euro. Phys. J. C **61**, 905 (2009).
- [27] L. D. Landau, Izv. Akad. Nauk SSSR, Ser. Fiz. **17**, 51 (1953).
- [28] J. D. Bjorken, Phys. Rev. D **27**, 140 (1983).
- [29] A. Dumitru, U. Katscher, J. A. Maruhn, H. Stocker, W. Greiner and D. H. Rischke, Z. Phys. A **353**, 187-190 (1995).
- [30] B. Schenke and M. Strickland Phys. Rev. D **76**, 025023 (2007).
- [31] P. Romatschke and M. Strickland, Phys. Rev. D **69**, 065005 (2004).
- [32] C. Song, Phys. Rev. C **47**, 2861 (1993).
- [33] S. Turbide, R. Rapp, and C. Gale, Phys. Rev. C **69**, 014903 (2004).
- [34] K. Kajantie, J. Kapusta, L. McLerran and A. Mekjian, Phys. Rev. D **34**, 2746 (1986).
- [35] A. Adare et al., PHENIX Collaboration, arXiv:0804.4168v1 [nucl-ex].

- [36] H. von Gersdorff, M. Kataja, L. McLerran, and P. V. Ruuskanen, Phys. Rev. D **34**, 794 (1986); *ibid* Phys. Rev D **34**, 2755 (1986).
- [37] S. Biswas et. al, in preparation.